Articles

Contribution from the Department of Chemistry,
University of California, Irvine, California 92717

Antiferromagnetic Exchange in an Isomorphous Series of Siloxy-Bridged Early-Transition-Metal Dimers: Comparisons of Antiferromagnetic Exchange Interactions in Isomorphous d^1–d^1, d^1–d^2, d^2–d^2, and d^2–d^3 Exchange-Coupled Dimers

Frank J. Feher* and John F. Walzer

Received February 1, 1989

The syntheses and characterization of several isomorphous siloxy-bridged dimers with the general formula $[(c\text{-}C_6H_{11})_7Si_7O_{12}M(C_5H_5N)_2][(c\text{-}C_6H_{11})_7Si_7O_{12}M']$ [**3a** (M = M' = Ti), **3b** (M = M' = V), **3c,d** (M ≠ M' = Ti, V), **3e** (M = Cr, M' = V)] are reported. The metal ions in these magnetically dilute complexes are strongly antiferromagnetically coupled. Temperature-dependent magnetic susceptibility measurements on dimers possessing either two Ti(III) ions or two V(III) ions indicate that the metal ions are strongly antiferromagnetically coupled ($-J > 1000$ cm^{-1} for **3a** and 80.5 cm^{-1} for **3b**). Attempts to prepare mixed-metal dimers containing one V(III) ion and either one Ti(III) or one Cr(III) ion led to solid solutions consisting of V(III)/V(III) dimers and either Ti(III)/V(III) or Cr(III)/V(III) dimers. Analysis of the temperature-dependent susceptibility data for these mixtures provided best-fit antiferromagnetic exchange constants ($-J$) of 187 and 55 cm^{-1}, respectively, for **3c,d** and **3e**. The observed correlation between $-J$ and the number of unpaired spins on each metal ion is discussed.

Polymetallic clusters of exchange-coupled first-row transition-metal ions have attracted widespread interest because of their relevance to magnetic materials and their importance in vital biological processes.[1] Many different exchange-coupled systems have been synthesized and studied in order to develop useful models for rationalizing and predicting the magnetic properties of these clusters.[2] Of particular interest have been bimetallic systems, which are generally the easiest to synthesize and the most amenable to detailed theoretical descriptions.[3]

Detailed studies on exchange-coupled bimetallics have provided great insight into the nature of magnetic interactions.[3] Unfortunately, there are very few series of bimetallic complexes that can be synthesized with enough structural and electronic similarities to permit accurate comparisons. From the standpoint of developing reliable theoretical models for the design of new materials with predictable magnetic behavior, it is important to develop syntheses of isomorphous compounds, where information about individual orbital parameters can be obtained with as many other factors as constant as possible.

We recently reported[4] the synthesis and characterization of **3a**, a siloxy-bridged dimer containing two Ti(III) ions. We now report that isomorphous V(III)/V(III), V(III)/Ti(III), and V(III)/Cr(III) complexes can also be synthesized (Scheme I). The trivalent transition-metal ions in these magnetically dilute, isomorphous complexes are strongly antiferromagnetically coupled and provide a unique opportunity for comparing magnetic exchange interactions in a series of complexes that nominally differ only in d^n electronic configurations (i.e., the identity of the metal).

Experimental Section

General experimental protocol and procedures for the synthesis of **1** are described in ref 5. $TiCl_3[N(CH_3)_2]_2$,[6a] $VCl_3[N(CH_3)_3]_2$,[6b] $V[N(SiMe_3)_2]_3$,[6c] $VCl_3(THF)_3$,[6d] and $CrCl_3[N(CH_3)_3]_2$[6e] were synthesized by using known procedures. Triethylamine (Et_3N) and pyridine were stirred over KOH pellets for several days and vacuum distilled (25 °C, 10^{-4} Torr) from CaH_2. Combustion (C, H) and atomic absorption analyses (V and/or Cr) were performed by Galbraith Laboratories (Knoxville, TN).

Synthesis of 3b. Solid $VCl_3[N(CH_3)_3]_2$ (71 mg, 0.258 mmol) was added to a solution of trisilanol **1** (250 mg, 0.257 mmol) in benzene (10 mL) containing 10% (v/v) Et_3N. After the solution was stirred for 15 min at 25 °C, the solvent was removed in vacuo (25 °C, 10^{-4} Torr). The blue residue was extracted with pentane, the mixture filtered to remove Et_3NHCl, and the solvent again removed in vacuo (25 °C, 10^{-4} Torr) to yield a dark blue amorphous solid, which was freely soluble (-40 to 25 °C) in most solvents with which it did not react. A small test tube containing a benzene solution of this blue material was lowered into a larger test tube containing 5 mL of 20% (v/v) pyridine in benzene. After the large tube was stoppered and allowed to stand 3–5 days, the large crystals of **3b** (204 mg, 72%) that had precipitated were collected on a fine-fritted funnel and washed with benzene. Anal. Calcd (found after benzene removal in vacuo) for $C_{94}H_{164}N_2O_{24}Si_{14}V_2$: C, 51.29 (49.66); H, 7.51 (7.41). UV-vis, [λ_{max}, nm (ϵ)]: 347 (1200), 360 (1200), 596 (720), 791 (295). Mp: 221–222 °C dec.

(1) Solomon, E. I.; Wilcox, D. E. In *Magneto-Structural Correlations in Exchange Coupled Systems*; Willet, R. D., Gatteschi, D., Kahn, O., Eds.; D. Reidel: Boston, MA, 1985; pp 463–96 and references cited therein.

(2) General reviews on exchange-coupled systems: (a) Carlin, R. L. *Magnetochemistry*; Springer-Verlag: New York, 1986. (b) Willet, R. D., Gatteschi, D., Kahn, O., Eds.; *Magneto-Structural Correlations in Exchange Coupled Systems*; D. Reidel: Boston, MA, 1985; pp 463–96 and references cited therein. (c) O'Connor, C. J. *Prog. Inorg. Chem.* **1982**, *29*, 203–83. (d) Hatfield, W. E. In *Theory and Applications of Molecular Paramagnets*; Boudreaux, E. A., Mulay, L. N., Eds.; Wiley-Interscience: New York, 1976; pp 394–449. (e) Ginsberg, A. P. *Inorg. Chim. Acta Rev.* **1971**, *5*, 45–68. (f) Sinn, E. *Coord. Chem. Rev.* **1970**, *5*, 313–47. (g) Ball, P. W. *Coord. Chem. Rev.* **1969**, *4*, 361–83. (h) Kokoszka, G. F.; Gordon, G. *Transition-Metal Chemistry* **1969**, *5*, 181–277. (i) Martin, R. L. In *New Pathways in Inorganic Chemistry*; Ebsworth, E. A. V., Maddock, A. G., Sharpe, A. G., Eds.; Cambridge University Press: London, 1968; pp 175–231. (j) Morrish, A. H. *Physical Principles of Magnetism*; Wiley: New York, 1965. (k) Goodenough, J. B. *Magnetism and the Chemical Bond*; Wiley: New York, 1963. (l) Anderson, P. A. In *Magnetism*; Rado, G. T., Suhl, H., Eds.; Academic Press: New York, 1963; p 25. (m) Anderson, P. A. *Solid State Phys.* **1963**, *14*, 99. (n) Kanamori, J. *J. Phys. Chem. Solids* **1959**, *10*, 87–98.

(3) Leading references on specific dimeric systems: (a) Messerle, L. *Chem. Rev.* **1988**, *88*, 1229–54. (b) Leuenberger, B.; Gudel, H. U. *Inorg. Chem.* **1986**, *25*, 181–4. (c) Hodgson, D. J. *Prog. Inorg. Chem.* **1977**, *23*, 173–241. (d) Jungst, R.; Sekutowski, D.; Davis, J.; Luly, M.; Stuckey, G. *Inorg. Chem.* **1977**, *16*, 1645–55. (e) Doedens, R. J. *Prog. Inorg. Chem.* **1976**, *21*, 209–76. (f) Hay, P. J.; Thibeault, J. C.; Hoffmann, R. *J. Am. Chem. Soc.* **1975**, *97*, 4884–99.

(4) Feher, F. J.; Gonzales, S. L.; Ziller, J. W. *Inorg. Chem.* **1988**, *27*, 3440–2.

(5) Feher, F. J.; Newman, D. A.; Walzer, J. F. *J. Am. Chem. Soc.* **1989**, *111*, 1741–8.

(6) (a) Fowles, G. W. A.; Hoodless, R. A. *J. Chem. Soc.* **1963**, 33–8. (b) Casey, A. T.; Clark, R. J. H.; Pidgeon, K. J. *Inorg. Synth.* **1973**, *13*, 179–81. (c) Bradley, D. C.; Copperthwaite, R. G. *Inorg. Synth.* **1978**, *18*, 112. (d) Mauzer, L. E. *Inorg. Synth.* **1981**, *21*, 135–140. (e) Duckworth, M. W.; Fowles, G. W. A.; Greene, P. T. *J. Chem. Soc. A* **1967**, 1592.

0020-1669/90/1329-1604$02.50/0

Scheme I

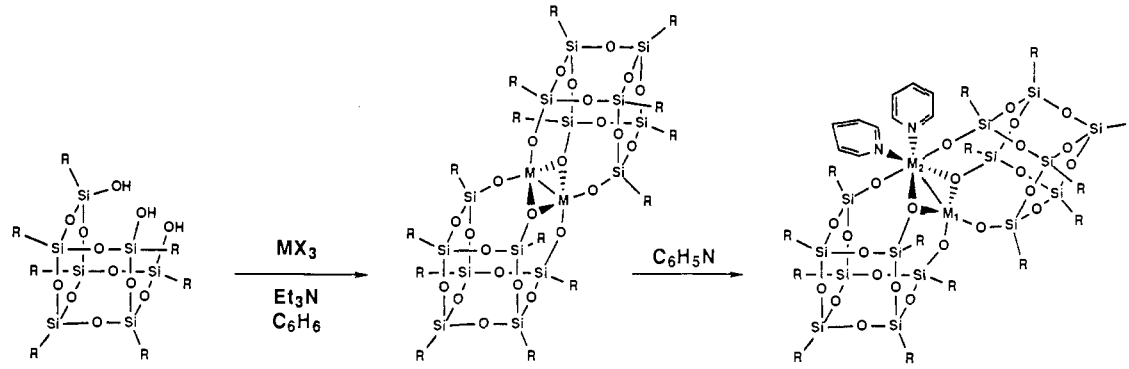

1 R = c-C_6H_{11} **2** M = Ti

	M_1 =	M_2 =
3a	Ti	Ti
3b	V	V
3c	Ti	V
3d	V	Ti
3e	V	Cr
3f	Cr	Cr

The use of $V[N(SiMe_3)_2]_3$ or $VCl_3(THF)_3$ instead of $VCl_3[N(CH_3)_3]_2$ had no noticeable effect on the outcome of the reaction.

Synthesis of Ti/V Mixed-Metal Dimers—Solid Solutions of 3a–c and/or 3d. (a) From 1:1 $VCl_3[N(CH_3)_3]_2$ and $TiCl_3[N(CH_3)_3]_2$. Solid $VCl_3[N(CH_3)_3]_2$ (53 mg, 0.192 mmol) was added with vigorous stirring to a solution of trisilanol **1** (372 mg, 0.205 mmol) in benzene (15 mL) containing 10% (v/v) Et_3N. Stirring for 10 min at 25 °C produced a dark purple solution, which quickly turned light blue upon the addition of solid $TiCl_3[N(CH_3)_3]$ (52 mg, 0.191 mmol). After the solution was stirred for 15 min at 25 °C, the solvent was removed in vacuo (25 °C, 10^{-3} Torr) to leave a blue residue. The residue was extracted with pentane and the mixture filtered to remove Et_3NHCl. Evaporation of the volatiles (25 °C, 10^{-4} Torr) gave a dark blue solid, which was freely soluble in most solvents with which it did not react. A benzene solution of the crude material in a small test tube was lowered into a larger test tube containing 5 mL of 20% (v/v) pyridine in benzene. After the large tube was stoppered and allowed to stand 3–5 days, the large crystals of mixed-metal dimer that precipitated (147 mg, 35%) were collected on a fine-fritted funnel and washed with benzene. Anal. Calcd (found after benzene removal in vacuo) for $C_{94}H_{164}N_2O_{24}Si_{14}TiV$: C, 51.32 (51.52); H, 7.53 (7.03). UV-vis [λ_{max}, nm (ϵ)]: 350 (120), 404 (sh, 180), 482 (450), 542 (sh, 300), 587 (sh, 170). Mp: 218–220 °C dec. Atomic absorption analysis of the sample after benzene removal in vacuo (Galbraith) found 2.32 ± 0.17% vanadium, which corresponds to 51.0 ± 3.7% of the metal sites being occupied by V(III) and 49 ± 3.7% of the sites being occupied by Ti(III).

(b) From 3:1 $VCl_3[N(CH_3)_3]_2$ and $TiCl_3[N(CH_3)_3]_2$. With use of the procedure described in part a, a sample of mixed-metal dimers was prepared from trisilanol **1** (1.00 g, 1.027 mmol), $VCl_3[N(CH_3)_3]_2$ (212 mg, 0.77 mmol), and $TiCl_3[N(CH_3)_3]_2$ (70 mg, 0.257 mmol). Atomic absorption analysis (Galbraith) of the sample found 3.66 ± 0.27% vanadium, which corresponds to 79 ± 6% of the metal sites being occupied by V(III).

Mixed-metal complexes containing Ti(III) and V(III) can also be prepared with $Ti[N(SiMe_3)_2]_3$[6c] instead of $TiCl_3[N(CH_3)_3]_2$. Interestingly, however, the use of $TiCl_3(THF)_3$,[6d] $VCl_3(THF)_3$,[6d] and/or the presence of THF in the reaction mixture leads to the formation of a black solid.

Synthesis of V/Cr Mixed-Metal Dimers—Solid Solutions of 3b and 3e. (a) From 1:1 $VCl_3(THF)_3$ and $CrCl_3[N(CH_3)_3]_2$. Solid $VCl_3(THF)_3$ (96 mg, 0.250 mmol) was added with vigorous stirring to a solution of trisilanol **1** (500 mg, 0.51 mmol) in benzene (15 mL) containing 10% (v/v) Et_3N. Stirring for 10 min at 25 °C produced a dark purple solution, which quickly turned light greenish blue upon the addition of solid $CrCl_3[N(CH_3)_3]_2$ (71 mg, 0.25 mmol). After the solution was stirred for 15 min at 25 °C, the solvent was removed in vacuo (25 °C, 10^{-3} Torr) to leave a blue residue. The residue was extracted with pentane and the mixture filtered to remove Et_3NHCl. Evaporation of the volatiles (25 °C, 10^{-4} Torr) gave a dark blue solid, which was freely soluble in most solvents with which it did not react. A benzene solution of the crude material in a small test tube was lowered into a larger test tube containing 5 mL of 20% (v/v) pyridine in benzene. After the large tube was stoppered and allowed to stand 3–5 days, the large crystals of mixed-metal dimer that precipitated (58 mg) were collected on a fine-fritted funnel and washed with benzene. Anal. Calcd (found after benzene removal in vacuo) for $C_{94}H_{164}N_2O_{24}Si_{14}TiV$: C, 51.32 (51.52); H, 7.53 (7.03). UV-vis [λ_{max}, nm (ϵ)]: 392 (128, sh), 428 (43, sh), 470 (38), 592 (210), 663 (17, sh), 802 (42). Mp: 224–225 °C dec. Atomic absorption (Galbraith) analysis of the sample after benzene removal in vacuo found 2.63 ± 0.10% vanadium and 1.59 ± 0.06% chromium, which corresponds to 62 ± 2.4% and 38 ± 1.4% of the metal sites being occupied by V(III) and Cr(III), respectively.

(b) From 1:1 $VCl_3[N(CH_3)_3]_2$ and $CrCl_3[N(CH_3)_3]_2$. With use of the procedure described in part a, a sample of mixed-metal dimers was prepared from trisilanol **1** (248 mg, 0.252 mmol), $VCl_3[N(CH_3)_3]_2$ (35 mg, 0.172 mmol), and $CrCl_3[N(CH_3)_3]_2$ (35 mg, 0.126 mmol). Atomic absorption analysis (Galbraith) of the sample after benzene removal in vacuo found 2.36 ± 0.10% vanadium and 1.96 ± 0.06% chromium, which corresponds to 55 ± 2.3% and 45 ± 1.4% of the metal sites being occupied by V(III) and Cr(III), respectively.

Analysis and Simulation of Magnetic Susceptibility Data. General Procedures. Magnetic data were collected from 15 to 300 K in a field of 10 kG on a SHE Model 905 SQUID susceptometer at the University of Southern California. The sample (25–40 mg) was finely pulverized, tightly packed into an aluminum sample bucket in a glovebox, and then inserted into the susceptometer by using standard Schlenk techniques. Temperature-dependent magnetic data for the various samples, including bucket correction terms (BC), sample magnetizations, and molar and inverse-molar susceptibilities (χ_M and $1/\chi_M$), are tabulated in Tables S1–S5 of the supplementary material.

Simulation of Magnetic Data. With an iterative procedure, the TIP, g value, exchange interaction constants, and composition of the sample were adjusted to minimize the sum of least-squares deviations between experimentally measured and calculated magnetization of the sample.[7] Any impurities were assumed to be identical with those of the sample, except that one atom was randomly oxidized to a d^0 ion (Ti for **3c,d** and V for **3b** and **3e**).

The calculated magnetization is represented by the equation

$$M_{calc} = BC + \sum_i M_i \qquad (1)$$

where $\sum M_i$ is the sum of magnetization due to the different dimers present in the sample and BC is the magnetization of the sample bucket, which was calculated from a fifth-order polynomial fit of 33 bucket magnetizations measured between 6 and 300 K. The total sample magnetization is given by

$$\sum_i M_i = \frac{G\cdot wt}{MW_{ave}} \sum_i [X_i(\chi_{M_i} + TIP_i + DMC_i)] + X_{imp}\left(DMC_{imp} - \frac{0.125g^2S(S+1)}{T}\right) \qquad (2)$$

where X_i is the mole fraction, χ_{M_i} is the molar susceptibility (metal atoms only), TIP_i is the temperature-independent paramagnetism, and DMC_i is the diamagnetic correction term for the i different d^n–d^m dimers in the

(7) A copy of the simulation program, written in complied BASIC for a Mac IIx computer, is available from the authors upon request.

sample. G is the field strength in gauss, wt is the mass of the sample in grams, and MW_{ave} is the average molecular weight of the sample (i.e., for nonstoichiometric metal ratios). For corrections due to paramagnetic impurities, X_{imp}, DMC_{imp}, g, and S are the mole fraction, diamagnetic correction term, g value, and total spin, respectively, for the impurity. T is the absolute temperature. The diamagnetic susceptibility of **1** was determined experimentally to be $(-6.11 \pm 0.14) \times 10^{-4}$ cgsu/mol.[4] Standard diamagnetic correction terms[8] were used for all other atoms and ligands. The percent purity referred to in the text represents the percentage of metal in the +3 oxidation state and equals $100(1 - X_{imp}/2)$.

The molar susceptibilities (χ_M) of the antiferromagnetically coupled d^n–d^m dimers (metal atoms only) were calculated by using the Van Vleck equation.[9] The molar susceptibility of the metal ions in **3b** is given by

$$\chi_M = \frac{Ng^2\beta^2}{kT}\left\{\frac{10 + 2\exp[-2J/kT]}{5 + 3\exp[-2J/kT] + \exp[(-3J + 3j)/kT]}\right\} \quad (3)$$

where $j = 0$ for the bilinear Heisenberg Hamiltonian ($\mathcal{H} = -J\langle S_1 \cdot S_2\rangle$) and $j > 0$ for the biquadratic Hamiltonian ($\mathcal{H} = -J\langle S_1 \cdot S_2\rangle + j\langle S_1 \cdot S_2\rangle^2$). For **3b** ($d^2$–$d^2$) a satisfactory fit of the experimental data could be obtained by using the bilinear Hamiltonian to model the metal–metal exchange interaction. (When the data for **3b** were simulated by using the biquadratic Hamiltonian, the best-fit j was zero.)

The experimental data for mixed-metal dimers containing Ti(III) and V(III) were simulated by using the best-fit J, TIP, and g values for **3a**[10] and **3b** to calculate the magnetization due to the d^1–d^1 and d^2–d^2 dimers in the mixture, which was subtracted from the experimentally measured sample magnetization. The difference, assumed to be due to **3c,d** or **3e**, was simulated as described below.

For d^1–d^2 dimers the mathematical expressions for the biquadratic and bilinear Hamiltonians are equivalent and only one parameter is required to fit the data.[11] The molar susceptibility of the metal ions in d^1–d^2 dimers is therefore given by

$$\chi_M = \frac{Ng^2\beta^2}{kT}\left\{\frac{5 + 0.5\exp[-1.5J/kT]}{4 + 2\exp[-1.5J/kT]}\right\} \quad (4)$$

The molar susceptibility of antiferromagnetically coupled d^2–d^3 dimers is given by

$$\chi_M = \frac{Ng^2\beta^2}{kT}\left\{\frac{17.5 + 5\exp[(-2.5J - 1.25j)/kT] + 0.5\exp[(-4J + 4j)/kT]}{6 + 4\exp[(-2.5J - 1.25j)/kT] + 2\exp[(-4J + 4j)/kT]}\right\} \quad (5)$$

where $j = 0$ for the bilinear Hamiltonian and $j > 0$ for the biquadratic Hamiltonian. Satisfactory fits of the experimental data for mixed d^2–d^2 and d^2–d^3 dimers could only be obtained when the biquadratic Hamiltonian was used to describe the exchange interaction in the d^2–d^3 dimer (i.e., **3e**).

Three different models were examined for the distribution of d^n and d^m ions in the mixed-metal samples. For the sake of discussion, it will be assumed that the percentage of sites occupied by the d^m ion is equal to or greater than the percentage of sites occupied by d^n ions.

Model 1. *All d^n ions are present as d^n–d^m dimers, and any remaining d^m ions are present as d^m–d^m dimers.* The d^n–d^n:d^m–d^m:d^n–d^m ratios of dimers are 0:[1 − 2(%d^n/100)]:[2(%d^n/100)], where %d^n is the percentage of sites occupied by the d^n metal. For mixed V(III)/Cr(III) samples, this model accurately predicts the experimental susceptibility data. For mixed Ti(III)/V(III) samples, however, this model produces totally unsatisfactory fits. Dimers **3c,d** possess an odd number of d electrons and exhibit large molar susceptibilities, especially at low temperature. The experimental susceptibilities of our mixed Ti(III)/V(III) sample decrease dramatically with temperature (Figure 2A), indicating that large proportions of the sample must consist of antiferromagnetically coupled dimers with even numbers of electrons (e.g., **3a** and **3b**).

Model 2. *All d^n and d^m ions are distributed as statistical mixtures of d^n–d^n, d^m–d^m, and d^n–d^m dimers.* The d^n–d^n:d^m–d^m:d^n–d^m ratios of dimers are $[(\%d^n/100)^2]$:$2((\%d^n \times \%d^m)/10^4)]$:$[(\%d^m/100)^2]$, where %$d^n$ and %d^m are the percentages of sites occupied by the d^n and d^m metal ions, respectively. This model also consistently failed to accurately simulate low-temperature (15–100 K) susceptibility data for mixed Ti(III)/V(III) dimers. At lower temperatures the calculated susceptibilities were progressively higher than the experimental data, indicating that the d^1–d^2 dimer constituted a smaller than statistical percentage of the sample. This model could not be applied to mixed V(III)/Cr(III) dimers because data for **3f** (the pure Cr(III)/Cr(III) dimer) were unavailable.

Model 3. *The d^n and d^m ions are distributed as nonstatistical mixtures of d^n–d^n, d^m–d^m, and d^n–d^m dimers.* With the mole fraction of d^n–d^n dimers represented as X, the maximum value for X is [1 − 2(100 − %d^n)/100] and the d^n–d^n:d^m–d^m:d^n–d^m ratios of dimers are X:[2(%d^n/100 − X)]:[1 − (%d^n/50) + X]. With this model the experimental susceptibility data for mixed Ti(III)/V(III) dimers could be accurately simulated.

The quality of the best-fit results obtained with all three models for mixed-metal dimers are very sensitive to the percentage of V(III) ions assumed to be present in the sample. The percentage of V(III) used in the simulation procedure was, therefore, allowed to iteratively vary within the 95% confidence limits of the atomic absorption analyses performed and specified by Galbraith Laboratories (Knoxville, TN). Summaries of the parameters used in our simulation procedure are collected in Table I.

X-ray Diffraction Study of 3b. Crystals suitable for an X-ray diffraction study were obtained by allowing pyridine to slowly diffuse into a benzene solution of the blue syrup obtained from the reaction of **1** with $VCl_3(NMe_3)_2$. Crystal data for **3b**·C_6H_6 solvate $[C_{94}H_{164}N_2O_{24}Si_{14}V_2 \cdot C_6H_6$ (fw 2279.5)] are as follows: monoclinic $C2/c$, $a = 27.287$ (5) Å, $b = 14.640$ (2) Å, $c = 31.149$ (4) Å, $\beta = 109.47$ (1)°; $V = 11732$ (3) Å^3; $D_{calc} = 1.291$ g/cm^3 ($Z = 4$). A total of 8273 unique reflections with $4.0 \le 2\theta \le 40.0°$ were collected on a Syntex $P2_1$ diffractometer at −60 °C with use of graphite-monochromated Mo Kα radiation. The structure was solved by direct methods (SHELXTL PLUS). Full-matrix least-squares refinement of positional and thermal parameters (anisotropic for Si, O, C, V, N) led to convergence with a final R factor of 0.081 for 623 variables refined against 4453 data with $|F_o| > 4.0\sigma(|F_o|)$. All other details regarding the crystal structure are reported in the supplementary material.

X-ray Diffraction Study of 3e (Containing 8.1% 3b). Crystals suitable for an X-ray diffraction study were obtained by allowing pyridine to slowly diffuse into a benzene solution of the greenish blue syrup obtained from the reaction of **1** with 0.5 equiv of $VCl_3(THF)_3$ and 0.5 equiv of $CrCl_3(NMe_3)_2$. Crystal data for **3e**·C_6H_6 solvate $[C_{94}H_{164}N_2O_{24}Si_{14}VCr \cdot C_6H_6$ (fw 2280.6)] are as follows: monoclinic $C2/c$, $a = 27.243$ (6) Å, $b = 14.591$ (3) Å, $c = 31.133$ (6) Å, $\beta = 109.51$ (2)°; $V = 11665$ (4) Å^3; $D_{calc} = 1.319$ g/cm^3 ($Z = 4$). A total of 5461 unique reflections with $4.0 \le 2\theta \le 45.0°$ were collected on a Syntex $P2_1$ diffractometer at −60 °C with use of graphite-monochromated Mo Kα radiation. The structure was solved by direct methods (SHELXTL PLUS). Full-matrix least-squares refinement of positional and thermal parameters (anisotropic for Si, O, V, Cr and isotropic for C, N) led to convergence with a final R factor of 0.112 for 383 variables refined against 3517 data with $|F_o| > 4.0\sigma(|F_o|)$. All other details regarding the crystal structure are reported in the supplementary material.

Results and Discussion

d^2–d^2 Dimers. The room-temperature reaction of **1** with 1 equiv of $V[N(TMS)_2]_3$ (TMS = trimethylsilyl), $VCl_3(THF)_3$, or $VCl_3(NMe_3)_2$ in benzene/triethylamine produces a deep blue solution. Evaporation of the volatiles (35 °C, 10^{-3} Torr), pentane extraction, and solvent removal in vacuo (25 °C, 0.1 Torr) affords a very air-sensitive dark blue oil. Repeated attempts to isolate a stable crystalline product from this oil were unsuccessful,[14] but

(8) Mulay, L. N. *Tech. Chem.* **1972**, *1* (4), 448–52.
(9) Van Vleck, J. H. *The Theory of Electric and Magnetic Susceptibilities*; Oxford University Press: Oxford, England, 1932.
(10) Inexplicably, the TIP for **3a** was incorrectly reported in ref 4. The correct value is 120×10^{-4} cgsu/mol of dimer.
(11) Mathematical expressions for the temperature dependence of the molar susceptibility for any d^1–d^n dimer derived by using both the bilinear and biquadratic Heisenberg Hamiltonians are equivalent. For d^1–d^2 dimers, the exponential term is $\exp(-1.5J/kT)$ for the bilinear Hamiltonian ($\mathcal{H} = -J\langle S_1 \cdot S_2\rangle$) and $\exp[(-1.5J' + 0.75j)/kT]$ for the biquadratic Hamiltonian ($\mathcal{H} = -J'\langle S_1 \cdot S_2\rangle + j\langle S_1 \cdot S_2\rangle^2$). Only one fitting parameter is required because $-1.5J$ can be used in place of $-1.5J' + 0.75j$.
(12) (a) Depending on the viewing angle, light transmitted through the crystal appears one of three different colors. The least intense colors are observed when crystals are viewed down the crystallographic 2-fold axis (i.e., the M–M bond). Pleochroic schemes for our samples are as follows. (b) **3a**: dark burgundy, light burgundy, very pale blue. (c) **3b**: dark green, blue-green, pale blue. (d) Solid solutions of **3a**, **3b**, and **3c,d** containing ~1:1 Ti/V: dark reddish brown, blue, pale green. (e) Solid solutions of **3b** and **3e** containing ~55:45 V/Cr: dark blue-green, blue, pale green.
(13) Fifteen well-centered reflections ($10 \le 2\theta \le 20°$) obtained from a poorly diffracting crystal of mixed-metal dimers containing ~1:1 Ti/V gave the following parameters for the monoclinic unit cell: $a = 27.110$ (13) Å, $b = 14.725$ (5) Å, $c = 31.145$ (12) Å, $\beta = 109.34$ (3)°, and $V = 11732$ (8) Å^3.

Table I. Final Iterative Least-Squares Simulation Data for **3b**, **3c,d**, and **3e**

	3b	**3c,d** (data from mixed Ti/V dimer contg 53.45% V)	**3c,d** (data from mixed Ti/V dimer contg 84.25% V)	**3e** (data from mixed V/Cr dimer contg 54.05% V)	**3e** (data from mixed V/Cr dimer contg 62.15% V)
		Iteration Limits			
$-J$, cm^{-1}	70–95 (0.5)	165–205 (1)	165–190 (1)	45–55 (0.5)	40–60 (0.5)
j, cm^{-1}				0–4 (0.1)	1.3[a,f]
TIP × 10^6, cgsu	0–400 (25)	0–300 (25)	75[a,c]	0–450 (50)	300[a,f]
g value	1.9–2.0 (0.01)	2.00[a,b]	2.00[a]	1.95[a,d]	1.95[a,d,f]
% purity	95–100 (0.05)	97.5–98.5 (0.05)	96–100 (0.1)	100.0[a,e]	100.0[a,e,f]
% V		52.0–53.5 (0.05)	83.0–85.0 (0.05)	53.6–54.15 (0.05)	60.5–62.2 (0.01)
% **3a** in sample		30.0–32.5 (0.1)	4.0–10.0 (0.5)		
		"Best-Fit" Data			
$-J$, cm^{-1}	80.5	187	176	51.0	46.0
j, cm^{-1}				1.3	1.3
TIP × 10^6, cgsu	250	75	75	300	300
g value	1.90	2.00	2.00	1.95	1.95
% purity	95.60	98.15	100.0	100.0	100.0
% V		53.45	84.25	54.05	62.15
% **3a** in sample		31.1	6.5		
quantity minimized[g]	χ	$1/\chi$	$1/\chi$	$1/\chi$	$1/\chi$
least-squares sum[h]	5.75 × 10^{-7}	79.3	404	15.6	171
correlation coeff[i]	0.9968	0.9985	0.9944	0.9995	0.9980

[a] No iterations were performed on this value. [b] Early iterative simulations consistently gave a g value of 2.00 for **3c,d**. Since the best-fit values for other parameters were essentially uneffected by changing g to 1.9, a constant value of 2.00 was used to reduce the time required for calculations. [c] Since the TIP represents a very small, almost negligible, portion of the total magnetization, the best-fit value obtained from the sample of mixed-metal dimers containing 53.45% V was used. [d] The quality of the best-fit is the same for g values between 1.9 and 2.0; therefore, a constant average value of 1.95 was used to reduce the time required for calculations. [e] Early iterative simulations could be consistently obtained without corrections for paramagnetic Curie law impurities; therefore, no iterations for purity were performed. [f] The best-fit value obtained from the sample of mixed-metal dimers containing 54.05% V was used. Since it is difficult to compare systems with two different biquadratic exchange constants (J and j), a constant value of 1.3 cm^{-1} was used. Allowing j to vary gave $-J$ = 45 cm^{-1} and j = 1.9 cm^{-1}. [g] χ represents minimization of $\sum(\chi_{exp} - \chi_{calc})^2$; $1/\chi$ represents minization of $\sum(1/\chi_{exp} - 1/\chi_{calc})^2$. [h] Represents the least-squares sum as defined by footnote g. [i] The correlation coefficient is $[N\sum xy - \sum x\sum y]/\{[N\sum x^2 - (\sum x)^2]^{1/2}[N\sum y^2 - (\sum y)^2]^{1/2}\}$, where N is the number of experimental points and $x = \chi_{exp}$ and $y = \chi_{calc}$ for minimization of χ or $x = 1/\chi_{exp}$ and $y = 1/\chi_{calc}$ for minimization of $1/\chi$.

the reaction of a dilute benzene solution of this material with pyridine vapor afforded high yields of **3b**.

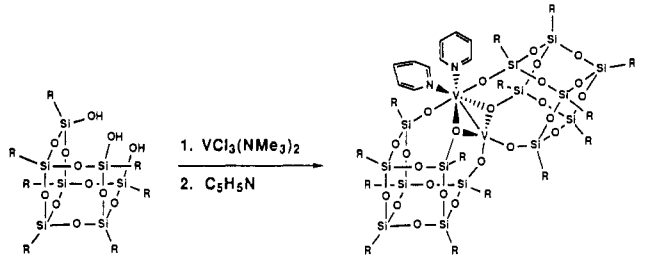

1 R = c-C_6H_{11} **3b**

Complex **3b**, like its Ti(III) analogue, is pleochroic[12] and insoluble in most solvents with which it does not react.[4] A preliminary determination of Laue symmetry, crystal class, and unit cell parameters indicated that **3b** was isomorphous with **3a**. This was later confirmed by a single-crystal X-ray diffraction study (vide infra).

The temperature-dependent molar susceptibility data for **3b** are shown in Figure 1. The experimental data are consistent with a strongly antiferromagnetically coupled $S_1 = S_2 = 1$ dimer and can be accurately simulated with the bilinear Heisenberg Hamiltonian ($\mathcal{H} = -J\langle S_1 \cdot S_2 \rangle$), with small corrections for temperature-independent paramagnetism (TIP) and $S = 1$ paramagnetic impurities. The best-fit values for J, the TIP, g value, and purity were −80.5 cm^{-1}, 250 × 10^{-6} cgsu/mol of dimer, 1.9, and 97.8%, respectively.

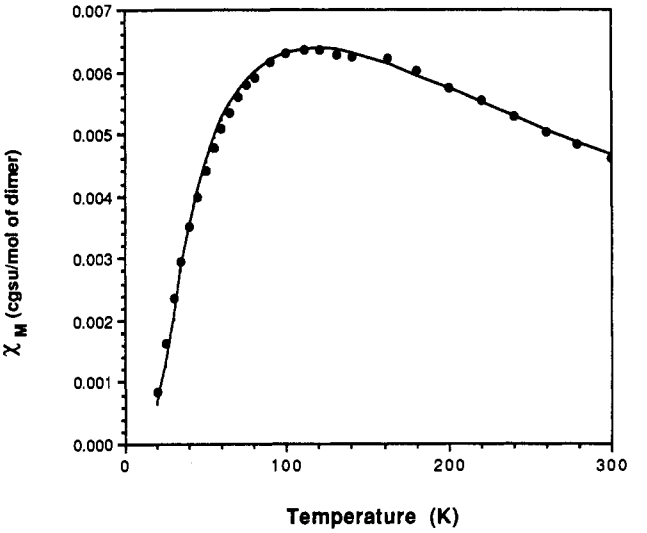

Figure 1. Experimental (●) and calculated (—) molar susceptibilities for **3b**. The "best-fit" line was calculated by using $-J$ = 80.5 cm^{-1}, TIP = 250 × 10^{-6} cgsu, and g = 1.90.

d^1–d^2 Dimers. The isomorphous relationship between **3a** and **3b** suggested that mixed-metal dimers containing both Ti(III) and V(III) could be synthesized. Indeed, when 2 equiv of trisilanol **1** was reacted sequentially with 1 equiv of $VCl_3(NMe_3)_2$ and 1 equiv of $TiCl_3(NMe_3)_2$, treatment of the resulting blue solution with pyridine afforded high yields of insoluble, pleochroic crystals containing both Ti and V. Our expectation that these crystals would be isomorphous with **3a** and **3b** was confirmed by a determination of Laue symmetry, crystal class, and unit cell parameters.[13]

Visible inspection of the mixed-metal sample suggested that it was a pure compound (e.g., **3c** or **3d**): the same characteristic

(14) (a) Based on our previous results[4] with **2** (M = Ti), which is poorly soluble in benzene and pentane unless there are traces of Et_3N present, we believe that the blue material is a bis(triethylamine) complex analogous to **3b**. In contrast to the titanium system, which upon standing at low temperature slowly dissociates Et_3N and crystallizes **2**, the vanadium system appears to be much more stable toward dissociation of Et_3N. On one occassion, however, the reaction of **1** with V[N-(SiMe$_3$)$_2$]$_3$ afforded small amounts of a poorly diffracting material that was isomorphous with **2** (M = Ti). As expected, this material was extremely soluble in benzene and pentane in the presence of small amounts of triethylamine. (b) We believe that the purple material is a pseudo-C_{3v} symmetric 2:1 adduct containing six-coordinate vanadium(III) ions.

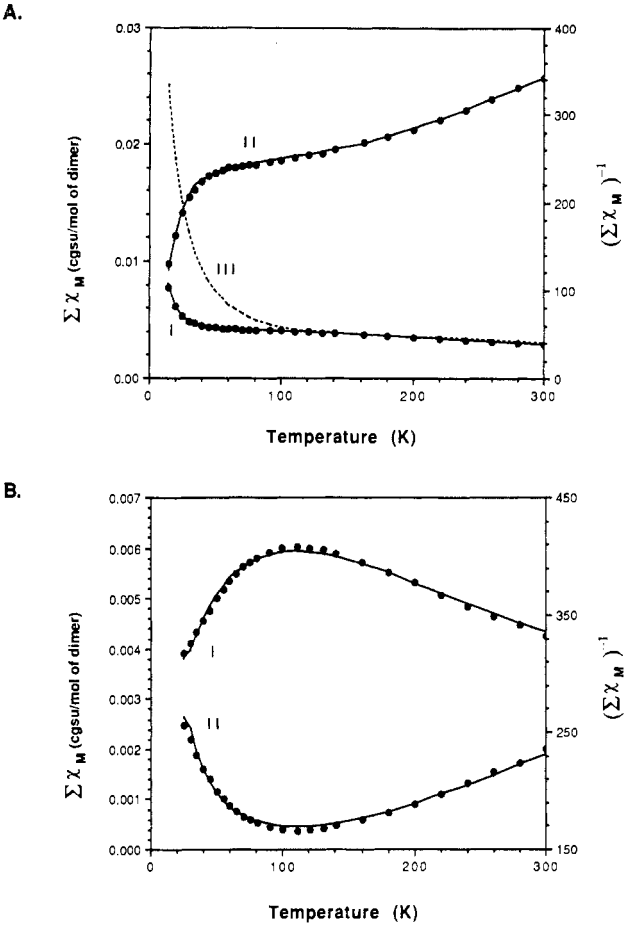

Figure 2. Calculated (●) and experimental (—) temperature-dependent molar susceptibility data for mixed-metal dimers containing Ti(III) and V(III). Curve I represents the sum of χ_M for all species (**3a–c** and/or **3d**) in the sample. Curve II is the inverse of curve I. Curve III is the expected behavior of a pure d^1–d^2 dimer (e.g., **3c** or **3d**) with $-J = 180$ cm^{-1}. (A) The "best-fit" lines were calculated for a 31.10:38.00:30.90 mixture of **3a**, **3b**, and **3c,d**. The parameters used to simulate magnetic data for **3c,d** were $-J = 187$ cm^{-1}, TIP = 75×10^{-6} cgsu, and $g = 2.0$. (B) The "best-fit" lines were calculated for a 7.0:74.50:18.50 mixture of **3a**, **3b**, and **3c,d**. The parameters used to simulate magnetic data for **3c,d** were $-J = 165$ cm^{-1}, TIP = 75×10^{-6} cgsu, and $g = 2.0$.

pleochroic behavior[12d] was observed for all crystals in the sample, and this was different from the pleochroic schemes observed for pure **3a**[12b] and pure **3b**.[12c] The temperature-dependent susceptibility data were not, however, consistent with a pure antiferromagnetically exchange-coupled d^1–d^2 dimer: the molar susceptibility of the sample at low temperatures was much too small for a complex containing an odd number of magnetically dilute d electrons (curve III in Figure 2A). Simulation of the experimental data (Figure 2A) could be accomplished by assuming that the sample was actually a random distribution (i.e., solid solution) of **3a–c** and/or **3d** containing 53.45% V(III) and 46.55% Ti(III) in the metal sites (Model 3). The best-fit J, TIP, and g value for **3c,d** were -187 cm^{-1}, 75×10^{-6} cgsu/mol of dimer, and 2.0, respectively. A small correction was also necessary for paramagnetic impurities (1.85%). At present we cannot determine whether **3c,d** or mixtures of both are responsible for the d^1–d^2 contribution to the total susceptibility of the sample. However, the fact that both Ti(III) and V(III) are capable of occupying the four- and six-coordinate sites in the lattice (i.e., both **3a** and **3b** exist), suggests that both **3c** and **3d** are present in the sample.

Homogeneous solid solutions containing variable amounts of Ti(III) and V(III) can be easily obtained by adjusting the relative proportions of $TiCl_3(NMe_3)_2$ and $VCl_3(NMe_3)_2$ used in the synthesis. The validity of our simulation procedure was therefore corroborated by preparing a mixed-metal sample containing 83.75% V(III) centers. Simulation of the experimental susceptibility data for this sample (Figure 2B), using the g value (2.0) and TIP (75×10^{-6} cgsu/mol) determined for the sample containing 46.55% Ti and 53.45% V, gave a best-fit J of -165 cm^{-1} for a solid solution of **3a** (7.00%), **3b** (74.50%), and **3c,d** (18.50%). Assuming that $-J$ lies somewhere between 165 and 187 cm^{-1}, these values fall within the range of experimental uncertainty for our analyses.

Numerous attempts were made to prepare pure samples of **3c** and/or **3d**, but in all cases homogeneous solid solutions were obtained. Several observations made during the course of these attempts suggest that disproportionation is extremely rapid and that any attempts to prepare pure **3c** or **3d** will lead to solid solutions of **3a–d**. First, the reactions of $VCl_3(NMe_3)_2/Et_3N$, $VCl_3(THF)_3/Et_3N$, or $V[N(TMS)_2]_3$ with 2 equiv of trisilanol **1** in benzene produce extremely air-sensitive purple solutions. The same purple color transiently appears upon the addition of $VCl_3(THF)_3$ or $VCl_3(NMe_3)_2$ to 1 equiv of **1** in Et_3N/benzene but quickly fades as the solution turns blue. Although efforts to obtain clean crystalline samples of either the blue or purple complexes have been unsuccessful due to their extremely high solubility in inert solvents and their sensitivity to traces of oxygen, reducible organics, and strongly coordinating ligands, the observation that blue solutions quickly turn purple upon the addition of 1 equiv of trisilanol/equiv of vanadium and purple solutions quickly turn blue upon the addition of 1 equiv of $VCl_3(NMe_3)_2$ or $V[N(TMS)_2]_3$ strongly suggests that the ratios of vanadium to trisilanol in the blue and purple complexes are 1:1 (or 2:2) and 1:2, respectively. Additional work is obviously required to unambiguously establish the structures of these complexes,[14] but the extreme ease with which their interconversion can be effected by the addition of **1** and/or other metal complexes (e.g., $VCl_3(NMe_3)_2$ or $V[N(TMS)_2]_3$) probably means that any attempt to prepare pure **3c** or **3d** will lead to disproportionation and the formation of solid solutions. Similar behavior is also observed by using $TiCl_3(NMe_3)_2$ or $Ti[N(TMS)_2]_3$, but the 1:2 Ti/trisilanol adduct appears to be inherently unstable and slowly decomposes upon standing.

d^2–d^3 Dimers. Mixed-metal dimers containing both V(III) and Cr(III) can be synthesized with $CrCl_3(NMe_3)_2$ and $VCl_3(NMe_3)_2$. When 2 equiv of trisilanol **1** was reacted sequentially with 1 equiv of $VCl_3(NMe_3)_2$ and 1 equiv of $CrCl_3(NMe_3)_2$, treatment of the resulting solution with pyridine afforded large, relatively air-stable, crystals that were isomorphous with **3a–d**. The same pleochroic behavior was observed for all crystals in the sample,[12e] but atomic absorption analyses of the vanadium and chromium content indicated a V:Cr ratio of approximately 55:45. Our suspicions that the sample was actually a solid solution of mixed V(III)/Cr(III) dimers were confirmed by temperature-dependent susceptibility studies.

The temperature dependence of χ_M and $1/\chi_M$ for a sample prepared by using 1:1 V(III)/Cr(III) is shown in Figure 3A. As was the case for V/Ti mixed-metal dimers, the experimental data are not consistent with a single antiferromagnetically exchange-coupled (d^2–d^3) dimer. Simulation of the experimental data could, however, be accomplished by assuming that the sample was a solid solution (Model 1) of **3b** (8.10%), and **3e** (91.90%). Using the bilinear Hamiltonian to model the exchange in **3e** produced mediocre fits, with a "best-fit" J of -55 cm^{-1}. Much better fits (curves I and II) were obtained with the biquadratic Hamiltonian ($\mathcal{H} = -J(S_1 \cdot S_2) + j(S_1 \cdot S_2)^2$) with $J = -51$ cm^{-1}, $j = 1.3$ cm^{-1}, and TIP = 300×10^{-6}.

Attempts to fit the susceptibility data by including contributions due to Cr/Cr dimer **3f** repeatedly gave unsatisfactory fits, indicating that there were negligible amounts of **3f** in the sample of mixed-metal V(III) and Cr(III) dimers. This interesting observation prompted us to check the validity of our simulation procedure by preparing a sample of mixed-metal dimers containing 61.65% vanadium sites. Simulation of the experimental susceptibility data (Model 1) for this sample (Figure 3B) by using the TIP and j obtained from the previous sample gave a best-fit J of -46 cm^{-1}, which was within experimental limit of error of the J obtained from the mixed-metal dimer containing 54.05% V(III) sites. As observed before, any attempt to include magnetic

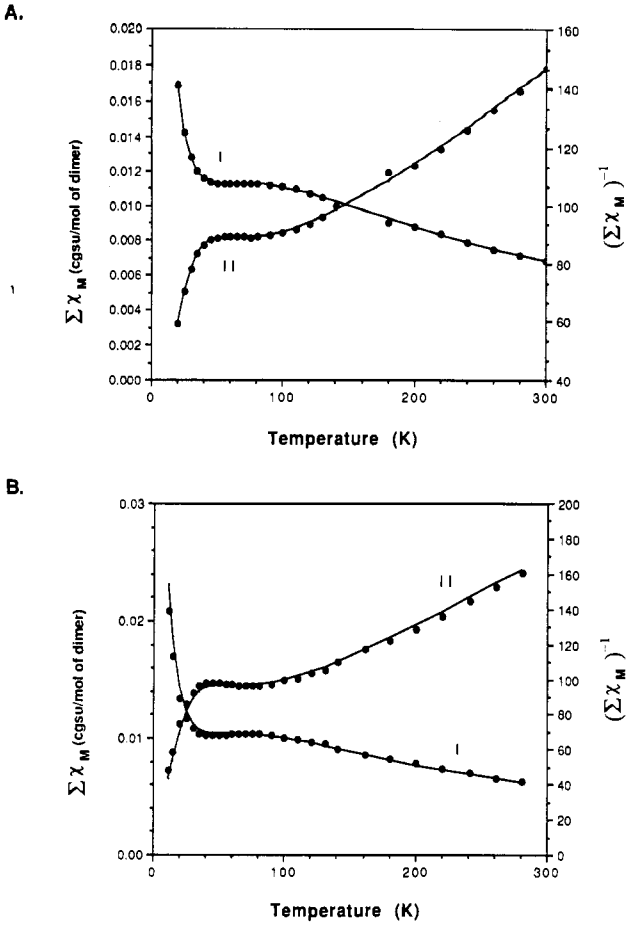

Figure 3. Calculated (●) and experimental (–) temperature-dependent molar susceptibility data for mixed-metal dimers containing V(III) and Cr(III). Curve I represents the sum of χ_M for all species (**3b** and **3e**) in the sample. Curve II is the inverse of curve I. (A) The "best-fit" lines were calculated for a 8.10:91.90 mixture of **3b** and **3e**. The parameters used to simulate magnetic data for **3e** were $-J = 51$ cm^{-1}, $j = 1.3$ cm^{-1}, TIP = 300×10^{-6} cgsu, and $g = 1.95$. (B) The "best-fit" lines were calculated for a 23.30:76.70 mixture of **3b** and **3e**. The parameters used to simulate magnetic data for **3e** were $-J = 46$ cm^{-1}, $j = 1.3$ cm^{-1}, TIP = 300×10^{-6} cgsu, and $g = 1.95$.

contributions due to **3f** produced much poorer fits of the experimental data.

It is clear from our susceptibility data that Cr(III)/Cr(III) dimer **3f** is not present to any significant extent in samples of V(III)/Cr(III) mixed-metal dimers. This presumably occurs because the strong preference of d^3 ions for octahedral coordination environments discourages the placement of Cr(III) ions in four-coordinate sites. The most likely structure for our V/Cr dimer is therefore **3e**, which places the d^3 and d^2 ion in energetically favorable octahedral and tetrahedral environments, respectively. Although all attempts to prepare pure **3e** have produced samples with more V(III) ions than Cr(III) ions, a single-crystal X-ray diffraction study on a mixed-metal sample containing 54.05% V and 45.95% Cr ions support our structural assignment for **3e** (vide infra).

Other Dimers? Efforts to extent this isomorphous series of siloxy-bridged dimers to include other trivalent ions were not successful. The reactions of **1** with a number of different Cr(III)-containing reagents failed to produce any isolable compound with a Cr:trisilanol ratio greater than 0.5, supporting our assertion that **3f** is thermodynamically unfavorable. Mixed Ti(III) and Cr(III) dimers would be of great interest but appear to be kinetically inaccessible and/or thermodynamically unstable due to electron transfer between the metal ions. Finally, several attempts to synthesize Fe(III)-containing dimers by using $FeCl_3$, $FeCl_3$(ligand) and $Fe[N(TMS)_2]_3$[6c] also led to complicated mixtures of inseparable products. In short, there does not appear to be immediate hope for synthesizing other M(III)/M′(III) dimers

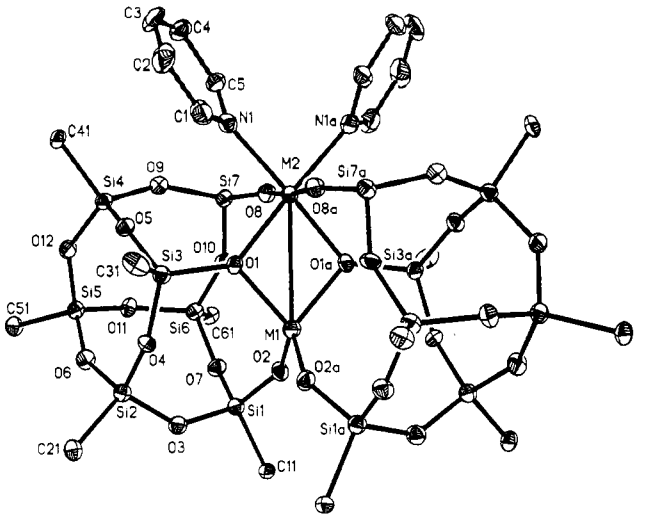

Figure 4. Perspective ORTEP plot of dimer **3b** (M(1) = M(2) = V), showing 20% probability thermal ellipsoids. For clarity only C atoms attached to Si atoms (except Si7) are shown.

Table II. Summary of Selected Bond Distances (Å) and Angles (deg) for **3a**, **3b**, and **3e** (Containing 8.1% of **3b**)

	3a [M(1 = M(2) = Ti]	**3b** [M(1) = M(2) = V]	**3e** [M(1) = V, M(2) = Cr]
M(1)–M(2)	2.901 (4)	3.039 (3)	3.015 (6)
M(1)–O(1)	1.990 (7)	1.950 (6)	1.952 (11)
M(1)–O(2)	1.829 (9)	1.819 (7)	1.854 (13)
M(2)–O(1)	2.070 (7)	2.047 (6)	2.026 (11)
M(2)–O(8)	1.916 (9)	1.894 (8)	1.895 (13)
M(2)–N(1)	2.247 (9)	2.162 (8)	2.122 (14)
Si(1)–O(2)	1.615 (9)	1.611 (7)	1.589 (14)
Si(3)–O(1)	1.631 (7)	1.648 (6)	1.634 (10)
Si(7)–O(8)	1.600 (9)	1.606 (8)	1.600 (14)
O(1)–M(1)–O(2)	113.2 (3)	118.2 (3)	119.7 (5)
O(1)–M(1)–O(1A)	91.0 (4)	83.4 (3)	83.3 (6)
O(2)–M(1)–O(2A)	115.5 (5)	110.6 (4)	108.7 (8)
O(1)–M(2)–N(1)	176.7 (3)	99.3 (3)	97.9 (5)
O(8)–M(2)–N(1)	87.3 (4)	88.0 (3)	87.5 (6)
O(1)–M(2)–O(1A)	86.6 (4)	78.7 (3)	79.6 (6)
N(1)–M(2)–N(1A)	79.9 (5)	82.7 (4)	84.6 (7)
M(1)–O(1)–M(2)	91.2 (3)	99.0 (2)	98.5 (4)
M(2)–O(8)–Si(7)	156.3 (4)	155.0 (4)	154.7 (6)
M(1)–O(2)–Si(1)	151.2 (5)	146.2 (4)	145.3 (6)

in the series by using other combinations of trivalent first-row transition metals. It may, however, be possible to synthesize isomorphous dimers by using combinations of V(IV) and divalent ions, such as Fe(II), Co(II), Ni(II), or Cu(II). This possibility is currently being explored.

Structural Considerations. Although **3a–e** are isomorphous, it is important to note that the distances and angles around the metal ions in the central M_2O_2 core are not equal. The ionic radii of the central metal ions decrease with increasing atomic number. Therefore, all atoms within the immediate coordination spheres of the metal ions must experience slight displacements within their lattice sites to accommodate changes in equilibrium bond lengths. To establish the magnitudes of the changes involved, single-crystal X-ray diffraction studies of **3b** and **3e** (containing 8.1% **3b**) were performed. A perspective ORTEP plot of the dimeric structure is shown in Figure 4. Selected distances and angles are collected in Table II, along with metrical data obtained from our previous study on **3a**.[4]

The most obvious trend in Table II is the decrease in the length of all bonds within the immediate coordination sphere of the metal ions as the large Ti(III) ions are replaced by smaller V(III) and Cr(III) ions. This is best illustrated by examining the M(2)–N distances, which vary from 2.247 (9) to 2.162 (8) to 2.122 (14) Å as M(2) changes from Ti(III) to V(III) to Cr(III). These bond length changes are comparable to the differences in covalent radii for Ti (1.32 Å), V (1.22 Å), and Cr (1.17 Å).[15] Similar trends

Table III. Best-Fit Exchange Constants and Selected Metrical Data for **3a–e**

	M(1)	M(2)	$-J$, cm^{-1}	M(1)–M(2), Å	M(1)–O–M(2), deg	O(1)–M(1)–O(1A), deg	O(1)–M(2)–O(1A), deg
3a	Ti	Ti	≥1000	2.901 (4)	91.2 (3)	91.0 (4)	86.6 (4)
3c,d	Ti(V)	V(Ti)	187				
3b	V	V	80.5	3.039 (3)	99.0 (2)	83.4 (3)	78.7 (3)
3e	V	Cr	55 ($-J$ = 51 and j = 1.3)	3.015 (6)	98.5 (4)	83.3 (6)	79.6 (6)

are observed for distances between M(2) and both O(1) and O(8). The M(1)–O(2) distances are surprisingly insensitive to the identity of the metal, but the nearly equal M(1)–O(1) distances in **3b** and **3e** are significantly shorter than those in **3a**. Although esd's for distances and angles in **3e** are somewhat high because of the presence of **3b** (8.1%) in the sample and isotropic refinement of thermal parameters for the cyclohexyl ring atoms, all of the structural data are consistent with our structural assignment for **3e**, which places the smaller Cr(III) ion in the six-coordinate site.

An inspection of Table II also indicates that the nearly square, crystallographically planar M_2O_2 core of **3a** undergoes substantial rhomboidal distortion as the Ti(III) ions are replaced by V(III) and/or Cr(III) ions. The O–M–O angles at both the four- and six-coordinate sites become 7–8° more acute as the metal ions are changed from titanium to chromium, and the M–O–M angles become corresponding more obtuse. Besides changing the M–O distances and angles in the M_2O_2 core, the effect of this distortion is to increase the metal–metal separation from 2.901 (4) Å in the case of **3a** to 3.039 (3) and 3.015 (6) Å in the cases of **3b** and **3e**, respectively.

As expected, the slight distortions of the coordination environments around the metal centers has very little effect outside of the immediate vicinity of the M_2O_2 core. Most of the other deviations are not statistically significant and would have negligible effects on the exchange interaction.

Comparisons of Exchange Interactions. The best-fit exchange constants for **3a**,[4,10] **3b**, **3c,d**, and **3e** are summarized in Table III, along with selected metrical data from Table II. For the sake of comparison the best-fit bilinear exchange constant for **3e** is included and a lower limit of 1000 cm^{-1} is used for $-J$ of **3a**. (Within experimental limit of error the susceptibility of **3a** is due solely to temperature-independent paramagnetism. There is, however, a curvature of the experimental susceptibility data (χ_M) toward higher values with increasing temperature that would be consistent with $-J \sim 1000$ cm^{-1}.)

It is clear from Table III that as the metal ions in the dimer are changed from Ti(III) to V(III) to Cr(III), the antiferromagnetic exchange constant ($-J$) decreases sharply. While this change is quite dramatic, much of it results simply from an increase in the number of unpaired d electrons associated with the ions. Decomposing J from the bilinear Hamiltonian into orbital contributions according to[16]

$$J = \frac{1}{n \cdot m}\sum_{ij} J_{ij}$$

$$J_{3a} = J_{11} \approx -1000\ \text{cm}^{-1}$$

$$J_{3c/3d} = \tfrac{1}{2}(J_{11} + J_{12}) = -188\ \text{cm}^{-1}$$

$$J_{3b} = \tfrac{1}{4}(J_{11} + J_{12} + J_{21} + J_{22}) = -80.5\ \text{cm}^{-1}$$

$$J_{3e} = \tfrac{1}{6}(J_{11} + J_{12} + J_{13} + J_{21} + J_{22} + J_{23}) \approx -55\ \text{cm}^{-1} \qquad (6)$$

where n and m are the number of unpaired electrons on each metal center and J_{ij} is the exchange integral $\langle\Phi_{Ai}(1)\Phi_{Bj}(2)|\mathcal{H}|\Phi_{Ai}(2)\Phi_{Bj}(1)\rangle$,[17] clearly shows that if only orbital contributions due to J_{11} are considered (i.e., only $J_{11} \neq 0$), the experimentally observed $-J$ for **3c,d**, **3b**, and **3e** should decrease by factors of 2, 4, and 6 relative to **3a**. To a first approximation, this is the trend that is experimentally observed. A similar trend is expected if the exchange parameter J is decomposed according to[3b,18]

$$J = -\frac{2}{n \cdot m}\sum_{\alpha\beta}\left(\frac{2}{U}A^2_{\alpha\beta} - B_{\alpha\beta\beta\alpha}\right) \qquad (7)$$

where $A_{\alpha\beta}$ is the transfer integral, $B_{\alpha\beta\beta\alpha}$ is the exchange integral, and U is the electron transfer energy.[19] Although variations in U and $A_{\alpha\beta}$ may obscure any regular trend, there is again an inverse dependence of J on the product of n and m, which is qualitatively observed with our experimental results.

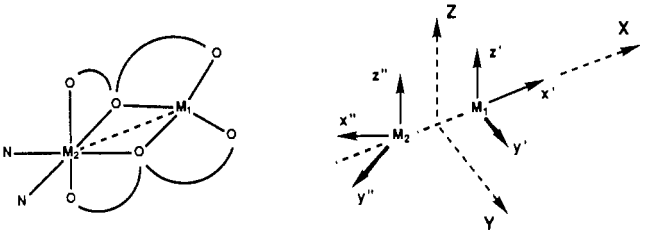

Figure 5. Schematic representation of the dimer framework and the local coordinate systems used to describe it.

It is tempting to rationalize part of the observed trend in terms of the relative importance of other orbital contributions to the overall exchange process. Unfortunately, any such rationalization would be complicated by the fact that the distances and angles around the metal ions in these isomorphous dimers are not equal: the nearly square M_2O_2 core of **3a** undergoes significant rhomboidal distortion as the metal ions are progressively changed from Ti to V to Cr. These changes are quite large and will undoubtedly have large effects on the relative magnitudes of the individual exchange parameters.

Detailed theoretical work will be required before meaningful comparisons can be made between the exchange parameters of **3a–e**. Nevertheless, two general observations can be made concerning the overall exchange parameters. First, it is clear that a large fraction of the changes observed in J are a consequence of the $1/nm$ dependence in the formula for J. This is particularly evident if **3a** is excluded from the comparison. Exchange parameters (J) for antiferromagnetically coupled dimers with more than one electron per ion are inherently much smaller than those observed for isomorphous Ti(III)–Ti(III) dimers. Second, the smallest M–O–M bond angle (91.2 (3)°) is observed for **3a**, the dimer with the largest exchange interaction ($-J \geq 1000$ cm^{-1}). The dominant mechanism for the exchange interaction therefore appears to be "direct exchange", since superexchange between two $d^n \leq 3$ ions is relatively inefficient and often ferromagnetic in nature when mediated by two atoms with bridging angles of ~90°.[2]

On the basis of the local coordinate systems shown in Figure 5, it is apparent that the d_{xy} orbital of a six-coordinate ion and the $d_{x^2-y^2}$ orbital of a four-coordinate ion are capable of overlapping when metal ions from edge-sharing octahedral ($d^n \leq 3$) and tetrahedral ($d^n \leq 2$) coordination environments are closely spaced.

(15) Dean, J. W., Ed. *Lange's Handbook of Chemistry*; McGraw-Hill: New York, 1985; pp 3-121–3-126.
(16) Briat, B.; Kahn, O.; Morgenstern-Badarau, I.; Rivoal, J. C. *Inorg. Chem.* **1981**, *20*, 4193–4220.
(17) Respectively, Φ_{Ai} and Φ_{Bj} are the magnetic orbitals around the two metal ions (A and B) and $\mathcal{H}$ is the electrostatic exchange Hamiltonian.[17]
(18) Leuenberger, G.; Gudel, H. U. *Mol. Phys.* **1984**, *51*, 1–20.
(19) For α and β, the orthonormal magnetic orbitals of monomer fragments A and B, the integrals $A_{\alpha\beta}$ (i.e., kinetic exchange) and $B_{\alpha\beta\beta\alpha}$ (i.e., potential exchange) are defined[18] as $\langle\alpha|\mathcal{H}|\beta\rangle$ and $\langle\alpha\beta|\mathcal{H}|\beta\alpha\rangle$, respectively, where $\mathcal{H}$ is the appropriate Hamiltonian for the magnetic orbitals of the system.

Orbitally similar situations occur in a number of other binuclear complexes (e.g., edged-sharing or confacial bioctahedral complexes,[2e,3b,16,20] dibridged trivalent titanocene complexes[3d]) where relatively large exchange interactions have been attributed to direct exchange between ions separated by ~3 Å or less. Since internuclear M-M separations in **3a-e** vary from 2.90 to 3.04 Å, strong direct exchange interactions seem highly probable.

Acknowledgment. We express our thanks and appreciation to Professor Christopher Reed (University of Southern California) for providing access to a SQUID susceptometer. We also thank Dr. Olivier Kahn for helpful suggestions. These studies were supported by the National Science Foundation (Grant CHE-8703016) and an NSF Presidential Young Investigator Award (Grant CHE-8657262). Funds for the purchase of the X-ray diffraction equipment were made available from NSF Grant CHE-85-14495. Financial support from the UCI Academic Senate Committee on Research is also gratefully acknowledged.

Supplementary Material Available: Magnetic data for **3b** and the Ti/V and V/Cr mixed-metal dimers, including temperature-dependent magnetizations, bucket correction terms (BC), sample magnetizations, and experimental and calculated molar and inverse-molar susceptibilities (χ_M and $1/\chi_M$) (Tables S1-S5), and X-ray crystal data for **3b** and **3e**, including textual summaries of experimental procedures and tables of crystal data, atomic coordinates, thermal parameters, bond lengths, and bond angles (Tables S6-S17) (29 pages); listings of calculated and observed structure factors for **3b** and **3e** (40 pages). Ordering information is given on any current masthead page.

(20) (a) Goodenough, J. B. *Phys. Rev.* **1960**, *117*, 1442-51. (b) Reference 2d, pp 382 and 398-99.

Contribution from the Chemistry and Materials Science Divisions, Argonne National Laboratory, Argonne, Illinois 60439, and Department of Chemistry, North Carolina State University, Raleigh, North Carolina 27695

Polymeric Anions Leading to Novel Packing Motifs in Donor-Radical Salts: Synthesis and Crystal and Band Electronic Structure of (BEDT-TTF)BiI_4

Urs Geiser,*,† Hau H. Wang,*,† Sandra M. Budz,† Michael J. Lowry,† Jack M. Williams,*,† Jinqing Ren,‡ and Myung-Hwan Whangbo*,‡

Received August 15, 1989

In an attempt to synthesize a 2:1 salt of bis(ethylenedithio)tetrathiafulvalene (BEDT-TTF or ET, $C_{10}H_8S_8$) with soft C—H···anion contacts, which promote an increase in the superconducting transition temperature, T_c, in β-$(ET)_2X$ salts, we carried out slow electrocrystallization of ET with BiI_3 and $[(n\text{-}C_4H_9)_4N]I$ in 1,1,2-trichloroethane. This led to an unexpected 1:1 salt, (ET)BiI_4, which was characterized by X-ray single-crystal diffraction. The polymeric anion, a $[BiI_4^-]_\infty$ chain, contains $[BiI_6]$ octahedra sharing edges, such that the two terminal iodide ligands are in a cis configuration. ET^+ cations form a network of $(ET^+)_2$ dimers, connected by S···S contacts shorter than the sum of the van der Waals radii (3.6 Å). The spin susceptibility as a function of temperature, derived from ESR measurements, follows Curie's law down to 20 K, but a spin count indicates that the ESR signal is due to an impurity (less than 1%). Band electronic structure calculations on the $(ET^+)_2$ layer predict (ET)BiI_4 to be a semiconductor with a band gap of order 0.4 eV. Crystal data: triclinic, space group $P\bar{1}$, lattice constants a = 8.265 (3) Å, b = 11.118 (3) Å, c = 14.424 (4) Å, α = 110.76 (2)°, β = 96.41 (2)°, γ = 103.57 (2)°, V = 1176.8 (7) Å^3, and Z = 2.

Bis(ethylenedithio)tetrathiafulvalene (BEDT-TTF or ET) is the most extensively used electron-donor molecule in the search for new organic superconductors.[1] At least ten ET-based ambient-pressure superconductors have been found to date, including that with the highest superconducting transition temperature, T_c, of any organic material, i.e., κ-$(ET)_2Cu(SCN)_2$, with T_c = 10 K.[2] Several structural families of superconducting ET salts exist, of which the best known is the β-$(ET)_2X$ group, where X can be a number of linear trihalide or dihalometalate anions, e.g., X^- = IBr_2^- (T_c = 2.8 K),[3] AuI_2^- (T_c = 4.9 K),[4] and I_3^- (T_c = 1.5,[5] 8 K).[6] The ET molecular packing arrangements, and hence the electrical properties, are largely determined by the size, shape, and charge distribution of the anions.

Structure-property correlations developed for the β-$(ET)_2X$ family of organic superconductors[1,7] indicated that large anions with polarizable end groups in general show more promise for the discovery of new superconductors. The late-period terminal halide ligands found in the large anions lead to soft C—H···X contacts, which correlate with T_c enhancement.[7] The iodine atom is the largest and most polarizable halogen atom, and its bonds with late-period main-group metals are among the longest covalent bonds known. In an attempt to synthesize a 2:1 salt of ET with soft C—H···I contacts, we carried out electrocrystallization of ET with bismuth iodide complex anions. This attempt led to an unexpected 1:1 salt, (ET)BiI_4, in which the counteranion exists as a $[BiI_4^-]_\infty$ chain. In the following we describe the synthesis,

Table I. Crystal and Refinement Parameters for (ET)BiI_4

$C_{10}H_8S_8BiI_4$	fw = 1101.25
a = 8.265 (3) Å	triclinic, space group $P\bar{1}$ (No. 2)
b = 11.118 (3) Å	T = 295 K
c = 14.424 (4) Å	λ = 0.71073 Å
α = 110.76 (2)°	ρ_{calcd} = 3.108 g cm^{-3}
β = 96.41 (2)°	μ = 133.5 cm^{-1}
γ = 103.57 (2)°	transm coeff = 0.246-0.646
V = 1176.8 (7) Å^3	$R(F_o)^a$ = 0.035
Z = 2	$R_w(F_o)^b$ = 0.032

$^a R = \sum||F_o| - |F_c||/\sum|F_o|$. $^b R_w = [\sum w(|F_o| - |F_c|)^2/\sum wF_o^2]^{1/2}$.

* To whom correspondence should be addressed.
† Argonne National Laboratory.
‡ North Carolina State University.

(1) Williams, J. M.; Wang, H. H.; Emge, T. J.; Geiser, U.; Beno, M. A.; Leung, P. C. W.; Carlson, K. D.; Thorn, R. J.; Schultz, A. J.; Whangbo, M.-H. *Prog. Inorg. Chem.* **1987**, *35*, 51.
(2) (a) Urayama, H.; Yamochi, H.; Saito, G.; Nozawa, K.; Sugano, T.; Kinoshita, M.; Sato, S.; Oshima, K.; Kawamoto, A.; Tanaka, J. *Chem. Lett.* **1988**, 55. (b) Gärtner, S.; Gogu, E.; Keller, H. J.; Klutz, T.; Schweitzer, D. *Solid State Commun.* **1988**, *65*, 1531. (c) Carlson, K. D.; Geiser, U.; Kini, A. M.; Wang, H. H.; Montgomery, L. K.; Kwok, W. K.; Beno, M. A.; Williams, J. M.; Cariss, C. S.; Crabtree, G. W.; Whangbo, M.-H.; Evain, M. *Inorg. Chem.* **1988**, *27*, 965.
(3) Williams, J. M.; Wang, H. H.; Beno, M. A.; Emge, T. J.; Sowa, L. M.; Copps, P. T.; Behroozi, F.; Hall, L. N.; Carlson, K. D.; Crabtree, G. W. *Inorg. Chem.* **1984**, *23*, 3839.
(4) Wang, H. H.; Beno, M. A.; Geiser, U.; Firestone, M. A.; Webb, K. S.; Nuñez, L.; Crabtree, G. W.; Carlson, K. D.; Williams, J. M.; Azevedo, L. J.; Kwak, J. F.; Schirber, J. E. *Inorg. Chem.* **1985**, *24*, 2465.

0020-1669/90/1329-1611$02.50/0